Indirect-Rotor-Field-Oriented-Control of a Double-Star Induction Machine Using the RST Controller.

R. N. Andriamalala, H. Razik
Université Henri Poincaré - Nancy 1
GREEN-UHP - UMR-7037, BP 239
F - 54506 Vandœuvre-lès-Nancy, Cedex, France
E-mail: [Rijaniaina.Andriamalala, Hubert.Razik]
@green.uhp-nancy.fr

F.M. Sargos
GREEN-ENSEM - UMR-7037
2 avenue de la Foret de Haye
F - 54516 Vandœuvre-lès-Nancy, Cedex, France
E-mail: Francois.Sargos@ensem.inpl-nancy.fr

***Abstract*—This paper focuses to apply the RST controller on the Indirect-Rotor-Field-Oriented-Control (IRFOC) of a Double Star Induction Machine (DSIM). After fixing the reference models, some algebraic conditions permits to design the current and speed controllers. This step consists to find three polynomials R, S, T of the controllers by solving the Diophante equation. The RST controllers can ensure robustness against uncertainties of mechanical and electrical parameters of the motor. It also offers further degrees of freedom upon the choice of the dynamic of the system. Simulations and analysis will be developed to prove the effectiveness of the study.**

I. Introduction

The dual-winding machines of various types become more attractive in industrial applications. Nevertheless, this concept is not really recent but have been introduced since the beginning of the last century [1]. The two categories of dual winding machine are the split-wound and self-cascaded one [1], [2]. In a split-wound machine, the stator winding is composed by two similar but separated three-phase windings wound with the same number of poles [1]. Both three-phase winding systems are supplied with the same frequency and the rotor is a classical squirrel cage. Due to its structure, the two stator windings are magnetically coupled. Moreover, high level of circulating currents may rise if the motor is supplied by an inverter [1], [3], [5]. Nonetheless, it is possible to noticeably attenuate this drawback by playing on the coil pitch because it has a great influence on the impedance value associated with circulating harmonic currents. Full pitch and special slot shape designs are also required to limit the magnitude of these circulating currents [4], [5]. The second possibility of reducing these circulating harmonics is the using of some special technics of PWM [6]. The second kind of dual winding machine is the self-cascaded one which was first suggested by Hunt in 1907 [1]. In order to incorporate the effects of a cascade connection, this kind of motor requires a special rotor structure formed by several nested loops. The two three phase winding may be wounded with two dissimilar pole numbers [7].

Some researches treat the application of the first category in the induction motors whose the two three-phase winding systems are electrically shifted by an angle α whose the most popular values are 0^o, 30^o, 60^o. The dual-phasing is a special case of multiphasing operation whose the main advantages are: a higher torque density for the same machine volume, reduced torque ripples, a greater fault tolerance and a higher reliability, the possibility to divide the controlled power on more inverter legs, it will reduce the current stress of each switch and the need for parallel and or series connection of semiconductor switches can be avoided [4]–[7].

There are several works on the vector control of the Double Star Induction Machine (DSIM). For example, the rotor-field-oriented control strategy of the motor was carried out by subdividing the system in two d, q sub-systems in the control [1], [8], [9]. It is even possible to enhance the torque density by injecting third harmonic component in the current reference because the fundamentals of the current and flux increase [9].

This paper mainly attempts to investigate the application of the RST controller in the indirect-rotor-field-oriented-control (IRFOC) of a DSIM whose both sub-stators are electrically shifted by an angle $\alpha = 60^o$. Nowadays, the RST controller is becoming widespread in electrical engineering application for advanced control such as in shunt and series active compensators used in power quality improvement [10]. Further theoretical investigations were developed for the calculation and design of this controller distinguishing the form of the system [11], [12]. After a description of the drive scheme deduced from the modeling, the controller calculation will be shown by fixing the poles of the current and speed loops. The knowledge of these poles allows to determine the three polynomials R,S,T by fixing additional algebraic constrains. Simulation developed with C++ software will be displayed to validate the study.

II. Drive scheme

Conventionally, the drive scheme is deduced from the modeling and the rotor field orientation condition. One

978-1-4244-1766-7/08/$25.00 ©2008 IEEE

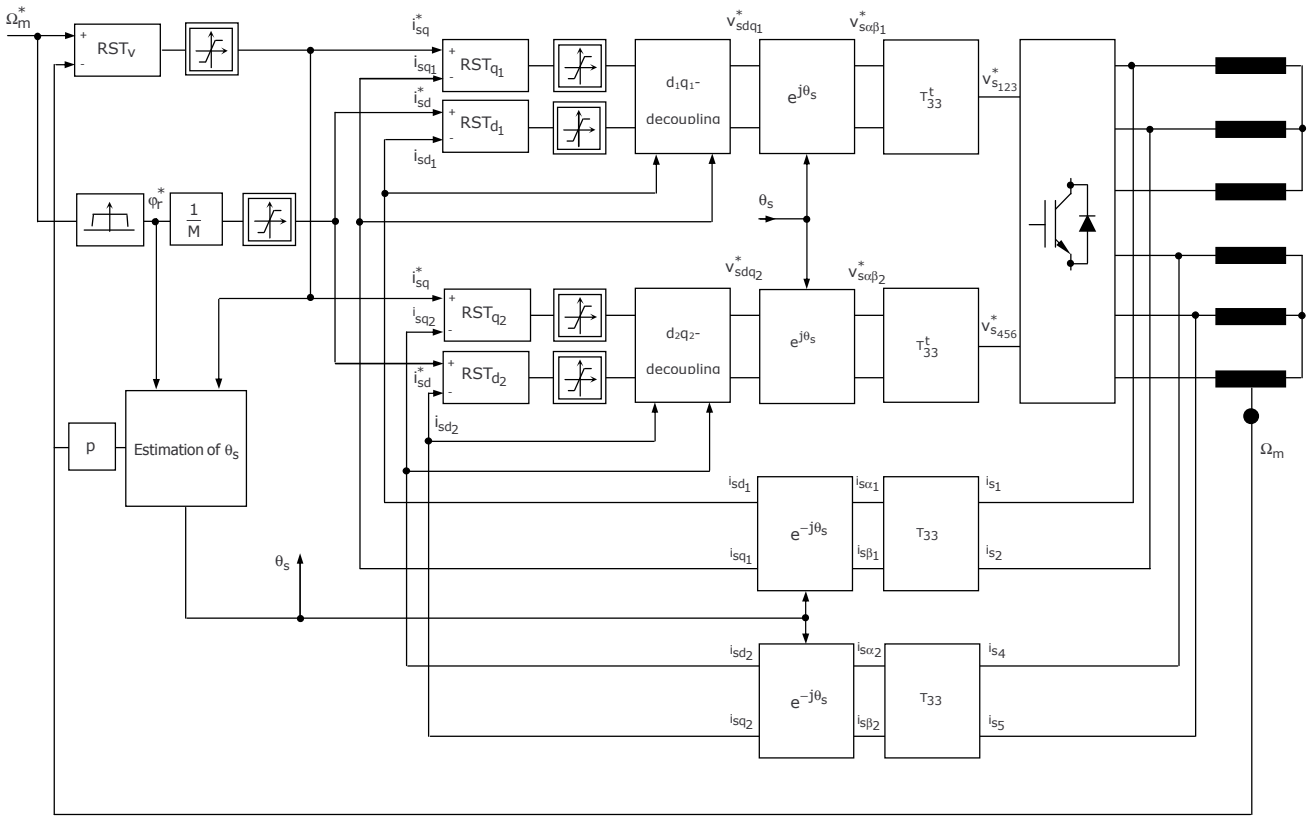

Fig. 1. The drive description

respectively applies the Concordia transformation and the Park rotation on each three phase sub-stator and rotor currents, voltages and flux. Let θ_s be the instantaneous position of the rotating field created by any phase of the first sub-stator. Since the second one is electrically shifted by an angle $\alpha = 60^o$, then the corresponding Park angle is $\theta_s - \alpha$. Taking into account all these considerations and choosing the sub-stator direct and quadrature currents i_{sd_1}, i_{sq_1}, i_{sd_2}, i_{sq_2}, the rotor direct and quadrature flux ψ_{rd}, ψ_{rq} as state variables, the model of the DSIM in the synchronous reference frame is:

$$\begin{cases} v_{sd_1} = R_s i_{sd_1} + \sigma L_s \frac{di_{sd_1}}{dt} + \sigma' L_m \frac{di_{sd_2}}{dt} + \frac{M}{L_r}\frac{d\psi_{rd}}{dt} \\ \qquad -\omega_s \left(\sigma L_s i_{sq_1} + \sigma' L_m i_{sq_2} + \frac{M}{L_r}\psi_{rq}\right) \\ v_{sq_1} = R_s i_{sq_1} + \sigma L_s \frac{di_{sq_1}}{dt} + \sigma' L_m \frac{di_{sq_2}}{dt} + \frac{M}{L_r}\frac{d\psi_{rq}}{dt} \\ \qquad +\omega_s \left(\sigma L_s i_{sd_1} + \sigma' L_m i_{sd_2} + \frac{M}{L_r}\psi_{rd}\right) \\ v_{sd_2} = R_s i_{sd_2} + \sigma L_s \frac{di_{sd_2}}{dt} + \sigma' L_m \frac{di_{sd_1}}{dt} + \frac{M}{L_r}\frac{d\psi_{rd}}{dt} \\ \qquad -\omega_s \left(\sigma L_s i_{sq_2} + \sigma' L_m i_{sq_1} + \frac{M}{L_r}\psi_{rq}\right) \\ v_{sq_2} = R_s i_{sq_2} + \sigma L_s \frac{di_{sq_2}}{dt} + \sigma' L_m \frac{di_{sq_1}}{dt} + \frac{M}{L_r}\frac{d\psi_{rq}}{dt} \\ \qquad +\omega_s \left(\sigma L_s i_{sd_2} + \sigma' L_m i_{sd_1} + \frac{M}{L_r}\psi_{rd}\right) \\ 0 = \frac{1}{\tau_r}\left[\psi_{rd} - M\left(i_{sd_1} + i_{sd_2}\right)\right] + \frac{d\psi_{rd}}{dt} - (\omega_s - p\Omega_m)\psi_{rq} \\ 0 = \frac{1}{\tau_r}\left[\psi_{rq} - M\left(i_{sq_1} + i_{sq_2}\right)\right] + \frac{d\psi_{rq}}{dt} + (\omega_s - p\Omega_m)\psi_{rd} \end{cases} \quad (1)$$

where v_{sd_1}, v_{sq_1}, v_{sd_2}, v_{sq_2} respectively indicate the direct and quadrature voltages of the first and second sub-stator. R_s, p, ω_s, Ω_m, respectively represent the stator resistance, the number of poles, the speed of the air-gap rotating field and the mechanical velocity of the motor. The inductances L_s, L_m, L_r, M are defined as follow:

$$\begin{cases} L_s = L_{sl} + 1.5L_{ms}, & L_m = 1.5L_{ms} \\ L_r = L_{rl} + 1.5L_{mr}, & M = 1.5M_{sr} \end{cases} \quad (2)$$

L_{sl}, L_{rl} are the stator and rotor leakage inductances. L_{ms}, L_{mr} are the stator and rotor self-magnetizing inductances. M_{sr} is the peak value of the stator-rotor mutual inductances. $\tau_r = L_r/R_r$ is the rotor time constant where R_r indicates the rotor resistance. Moreover, $\sigma = 1 - \frac{M^2}{L_s L_r}$ $\sigma' = 1 - \frac{M^2}{L_m L_r}$. The electromagnetic torque is:

$$T_{em} = pM\left[(i_{sq_1} + i_{sq_2})\psi_{rd} - (i_{sd_1} + i_{sd_2})\psi_{rq}\right] \quad (3)$$

The IRFOC consists to make $\psi_{rq} = 0$ while the rotor direct flux ψ_{rd} converges to the reference ψ_r^*. The rotor flux becomes independent from i_{sq_1} and i_{sq_2} while the motor torque will be proportional to $i_{sq_1} + i_{sq_2}$. The only degree of freedom is the air-gap rotating field speed ω_s which must be used to regulate ψ_{rq} to zero. According to (1), in order to achieve this condition, the stator voltage angular frequency ω_s is instantaneously defined by the relation:

$$\omega_s = p\Omega_m + \frac{M}{\tau_r}\frac{i_{sq_1}^* + i_{sq_2}^*}{\psi_r^*} \quad (4)$$

Both sub-stators are identical. Hence, one can impose

$i^*_{sq_1} = i^*_{sq_2} = i^*_{sq}$ and $i^*_{sd_1} = i^*_{sd_2} = i^*_{sd}$, with:

$$i^*_{sq} = \frac{T^*_{em}}{2pM\psi^*_r} \tag{5}$$

Referring again to (1), the d_1-axis circuit is magnetically coupled with the d_2, q_1 and q_2-axis one respectively through the terms $\sigma \cdot L_m di_{sd_2}/dt$, $-\omega_s \sigma L_s i_{sq_1}$ and $-\omega_s \sigma \cdot L_m i_{sq_2}$. Analog magnetic couplings exist for d_2, q_1 and q_2-axis circuits. A decoupling algorithm is then needed in the control. It may be static or dynamic. To simplify, the authors utilize the static one in this paper. In the algorithm, the derivative of any current can be replaced by the ratio between its variation with the electrical sampling time T_e. For instance, $\sigma \cdot L_m di_{sd_2}/dt$ can be approximated by $\sigma \cdot L_m \Delta i_{sd_2}/T_e$. The drive scheme is summarized by the figure (1).

III. Controller calculations

A. Current Controller

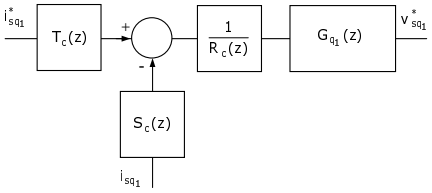

Fig. 2. The RST controller of the current loops

The goal of this section to determinate the RST current controller constituted by the three polynomials $R_c(z)$, $S_c(z)$, $T_c(z)$ and illustrated by the figure (2). The relation (1) allows to calculate the discrete transfer function of each current loop is:

$$H_c(z) = \frac{B_c(z)}{A_c(z)} = \frac{b_{0c}}{z + a_{0c}} \tag{6}$$

such that:

$$a_{0_c} = -e^{-\frac{T_e}{\sigma\tau_s + \tau_d}}, \qquad b_{0_c} = \frac{1}{R_s}\left(1 + a_{0_c}\right) \tag{7}$$

where, T_e designates the electrical sampling time which is equal to $200\mu s$. $\tau_s = L_s/R_s$. $\tau_d = 300\mu s$ is the overall delay introduced by the hardware system. For this study, the index c indicates a symbol related to the current of the $d_1 - q_1$ and $d_2 - q_2$ axis. Reference [11] affirms that with the controller RST, the overall system transfer function $H_{mc}(z)$ is given by

$$H_{mc}(z) = \frac{B_{mc}(z)}{A_{mc}(z)} = \frac{T_c(z)B_c(z)}{A_c(z)R_c(z) + B_c(z)S_c(z)} \tag{8}$$

The index m means a symbol related of the tracked model. For simplification, the polynomial $A_{mc}(z)$ must be monic [11]. The knowledge of degrees $d^oA_c(z)$, $d^oB_c(z)$, $d^oA_{mc}(z)$ and $d^oB_{mc}(z)$ of the afore-mentioned polynomials permits to define them. For simplification reason, one can set $d^oA_{m_c} - d^oB_{m_c} = d^oA_c - d^oB_c$. Furthermore, for the tracked transfer function $H_{mc}(z)$, one has degrees of freedom, so it is advantageous that may be third or second. For exemple, the authors fixe a second order i.e $A_{mc}(z) = z^2 + a_{m_{1c}}z + a_{m_{0c}}$. The coefficients $a_{m_{1c}}$, $a_{m_{0c}}$ depends on the pole placement. A possible solution for pole assignment is the emulation technic which consists to design the poles in the continuous domain and to find the equivalent poles in the discrete one. It is also possible to utilize the root locus in the z-plane [11].

Let z_{1c} and z_{2c} be these poles in the discrete domain. Hence:

$$a_{m_{0c}} = z_{1c}z_{2c}, \qquad a_{m_{1c}} = -z_{1c} - z_{2c} \tag{9}$$

B_{mc} must be designed to ensure the condition $\lim_{z\to 1} H_{mc}(z) = 1$. This condition allows to determinate $B_{mc}(z)$:

$$B_{mc}(z) = 1 - z_{1c} - z_{2c} + z_{1c}z_{2c} \tag{10}$$

Moreover, it is advantageous to introduce additional integral in the controller to cancel an eventual steady-state error $R_c(z) = (z-1)R'_c(z)$, both $R_c(z)$ and $R'_c(z)$ are monic. Furthermore, for causality, the degrees of $S_c(z)$ and $T_c(z)$ must be no greater than that of $R_c(z)$ [11]:

The polynomial $T_c(z)$ can be designed by the expression below:

$$T_c(z) = \frac{A_{mc}(1)}{B_c(1)}A_{0c}(z) \qquad \text{with} \qquad A_{0c}(z) = z^k \tag{11}$$

k can be calculated as follow:

$$k = 2d^oA_c - d^oA_{mc} = 0 \Longrightarrow A_{0c}(z) = 1 \tag{12}$$

Therefore, $T_c(z)$ is constant:

$$T_c(z) = \left(\frac{1 - z_{1c} - z_{2c} + z_{1c}z_{2c}}{1 - e^{-\frac{T_e}{\sigma\tau_s + \tau_d}}}\right) R_s \tag{13}$$

Further algebraic considerations permit to point out the shapes of the polynomials $R_c(z)$ and $S_c(z)$ which are:

$$R_c(z) = z - 1 \qquad S_c(z) = s_{0c} + s_{1c}z \tag{14}$$

Solving the Diophante equation allows to find the coefficients s_{0c} and s_{1c}:

$$(z-1)A_c(z) + B_c(z)S_c(z) = A_{mc}(z)A_{0c}(z) \tag{15}$$

They are given by the relations:

$$\begin{cases} s_{0c} = \left(\frac{z_{1c}z_{2c} - e^{-\frac{T_e}{\sigma\tau_s + \tau_d}}}{1 - e^{-\frac{T_e}{\sigma\tau_s + \tau_d}}}\right) R_s \\ \\ s_{1c} = \left(\frac{1 - z_{1c} - z_{2c} + e^{-\frac{T_e}{\sigma\tau_s + \tau_d}}}{1 - e^{-\frac{T_e}{\sigma\tau_s + \tau_d}}}\right) R_s \end{cases} \tag{16}$$

B. Speed Controller

The velocity discrete transfer function is:

$$H_v(z) = \frac{b_{0v}}{(z + a_{0v})} \tag{17}$$

with:

$$a_{0v} = -e^{-f_v\frac{T_m}{J}} \qquad b_{0v} = \frac{1}{f_v}\left(1 + a_{0v}\right) \tag{18}$$

f_v and J respectively designate the viscous friction coefficient and the inertia. $T_m = 1ms$ indicates the mechanical sampling time. These informations indicates that the speed transfer function is also first order. Therefore, the controller design is identical than that of the current. Let z_{1v} and z_{2v} be the poles of the discrete tracked model, the polynomials $R_v(z)$, $S_v(z)$, $T_v(z)$ of the speed controller are:

$$\begin{cases} R_v(z) = z - 1 \\ S_v(z) = s_{0v} + s_{1v} z \\ T_v(z) = t_{0v} \end{cases} \quad (19)$$

such that:

$$\begin{cases} s_{0v} = \left(\frac{z_{1v} z_{2v} - e^{-f_v \frac{T_m}{J}}}{1 - e^{-f_v \frac{T_m}{J}}} \right) f_v \\ s_{1v} = \left(\frac{1 - z_{1v} - z_{2v} + e^{-f_v \frac{T_m}{J}}}{1 - e^{-f_v \frac{T_m}{J}}} \right) f_v \\ t_{0v} = \left(\frac{1 - z_{1v} - z_{2v} + z_{1v} z_{2v}}{1 - e^{-f_v \frac{T_m}{J}}} \right) f_v \end{cases} \quad (20)$$

IV. Simulation Results

One has released the experimental results using a double-star induction machine. Electrical parameters and technical details of the motor are summarized by the table I below.

TABLE I
MACHINE PARAMETERS

Nominal frequency	50	Hz
Nominal voltage	127	V
Nominal power rating	3	kW
Angle between both sub-stators α	$\pi/3$	rd
Stator resistance R_s	7.0	Ω
Rotor resistance R_r	2.40	Ω
Stator leakage inductance L_{sl}	0.010	H
Rotor leakage inductance L_{rl}	0.010	H
Stator magnetizing inductance L_{ms}	0.397	H
Rotor magnetizing inductance L_{mr}	0.397	H
Peak of the mutual stator rotor M_{sr}	0.3914	H
Inertia J	0.0329	$kg.m^2$
Viscous friction f_v	0.0040	Nms/rd
Number of poles $2p$	2	

In figures (3) and (4), the d_1 and q_1-axis current responses of the first sub-stator (or star) are sketched while in the figures (5) and (6), the d_2 and q_2-axis current responses of the second star are displayed. Figure (7) sketches the trace of the phase current while figure (11) indicates the dynamic behavior of the mechanical speed.

At the beginning, the DSIM is running at $-600rpm$. At $t = 3s$, one reverses the speed reference from $-600rpm$ to $600rpm$, according to figures (3), (4), (5) and (6) the current controllers successfully react to track references i^*_{sd}, i^*_{sq}. The zoom of the phase current around this instant in figure (8) confirms again quick reaction of current controllers to track its reference. Figure (11) of the speed and its reference also shows that the controller RST provides satisfactory result because the response is fast and there is no static error.

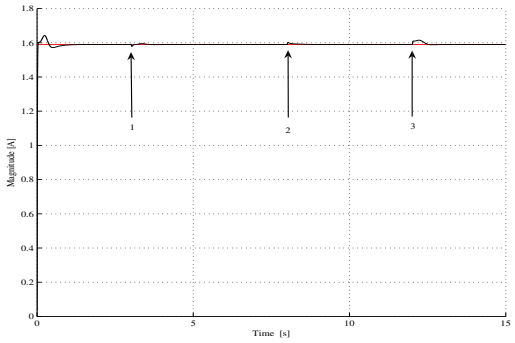

Fig. 3. Transient behavior of the direct current i_{sd_1} (black) of the first star and its reference i^*_{sd} (red): (1)-speed reversal from -600 rpm to 600rpm, (2)-step to 50% of the nominal load, (3)-load step to the nominal and speed step to 1200 rpm.

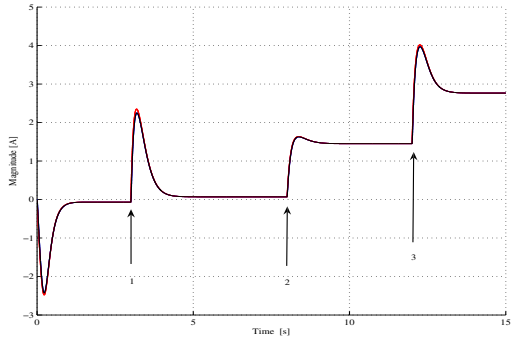

Fig. 4. Transient behavior of the direct current i_{sq_1} (black) of the first star and its reference i^*_{sq} (red): (1)-speed reversal from -600 rpm to 600rpm, (2)-step to 50% of the nominal load, (3)-load step to the nominal and speed step to 1200 rpm.

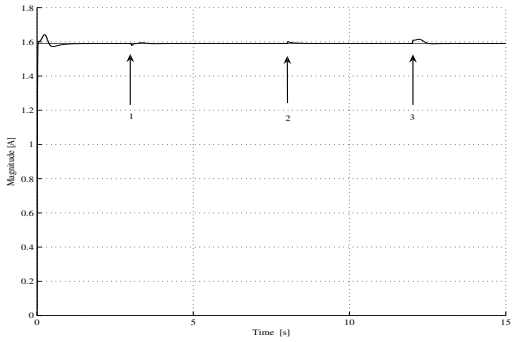

Fig. 5. Transient behavior of the direct current i_{sd_2} (black) of the second star and its reference i^*_{sd} (red): ((1)-speed reversal from -600 rpm to 600rpm, (2)-step to 50% of the nominal load, (3)-load step to the nominal and speed step to 1200 rpm.

At $t = 8s$, let us step the load of the motor at 50% of the nominal, figure (11) confirms again a successfully disturbance rejection by the speed controller. As it is stated in figures (4) and (6), the DSIM develops the needed torque for this load level. Once more, figure (9) zooming the phase current around this moment confirms the reliability of the RST current controllers.

978-1-4244-1766-7/08/$25.00 ©2008 IEEE

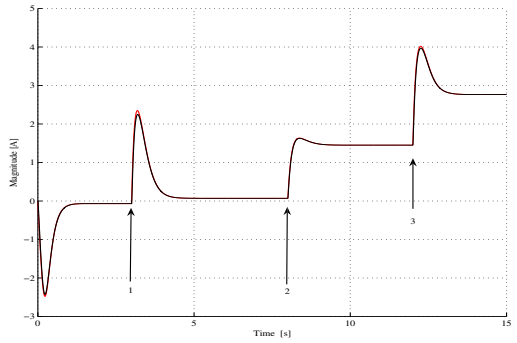

Fig. 6. Transient behavior of the quadrature current i_{sq_2} (black) of the second star and its reference i^*_{sq} (red): (1)-speed reversal from -600 rpm to 600rpm, (2)-step to 50% of the nominal load, (3)-load step to the nominal and speed step to 1200 rpm.

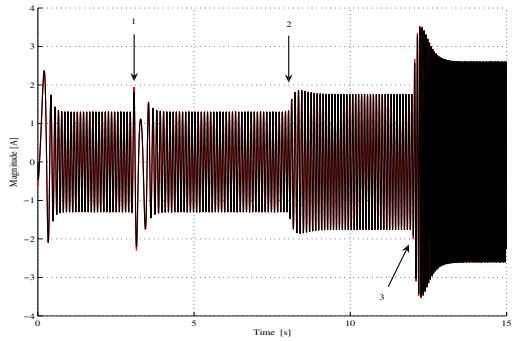

Fig. 7. Transient behavior of the current of the first star i_{sb_1} (black) and its reference $i^*_{sb_1}$ (red): (1)-speed reversal from -600 rpm to 600rpm, (2)-step to 50% of the nominal load, (3)-load step to the nominal and speed step to 1200 rpm.

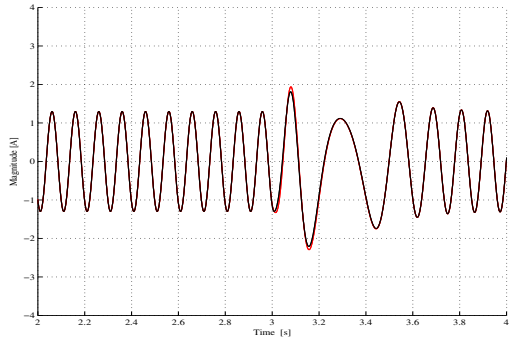

Fig. 8. Zoom of the phase current i_{sb_1} (black) and its reference $i^*_{sb_1}$ (red) while reversing the speed.

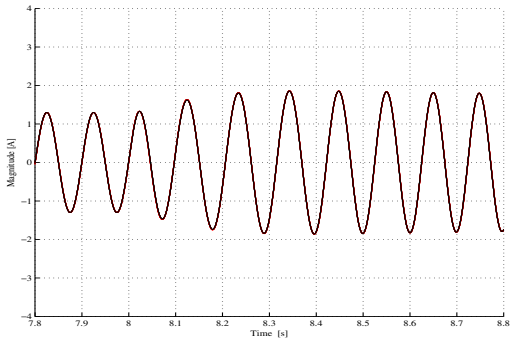

Fig. 9. Zoom of the stator phase current i_{sb_1} (black) and its reference $i^*_{sb_1}$ (red) while stepping the load to 50% of the nominal load.

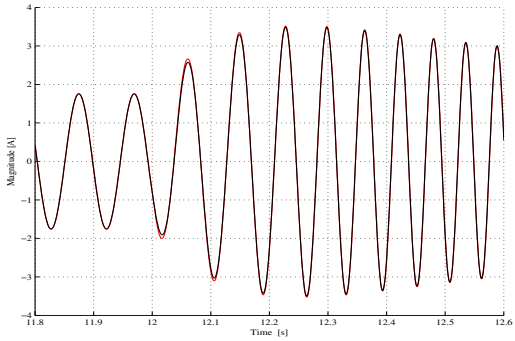

Fig. 10. Zoom of the stator phase current i_{sb_1} (black) and its reference $i^*_{sb_1}$ (red) while stepping the load to the nominal and the speed to 1200 rpm.

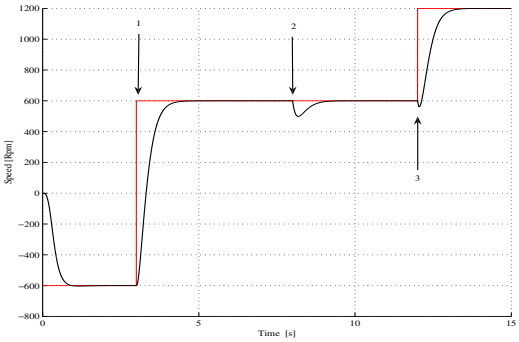

Fig. 11. Dynamic behavior of the speed: (1)-speed reversal from -600 rpm to 600rpm, (2)-step to 50% of the nominal load, (3)-load step to the nominal and speed step to 1200 rpm.

The ultimate case is done at the instant $t = 12s$ by stepping simultaneously the load level and the speed to the nominal and to $1200rpm$, respectively. Figures (3), (4), (5), (6), (10) and (11) indicate again correct actions of the current and speed controllers to reject disturbance and to ensure the tracking of references.

To test robustness of RST controllers against uncertainties of electrical and mechanical parameters of the DSIM, we simultaneously introduce variations of 20% on the stator self-magnetizing inductance, of $+80\%$ on the viscous friction and of -50% inertia when calculating the controllers. The motor is loaded at the nominal and starts up to $-1200rpm$. Figures (12), (13) one the motor successfully starts up to $-1200rpm$ with no steady-state error in the stator currents and mechanical speed. By setting a reversal speed at $t = 3s$, one notes that current and speed controllers ensure good tracking. Therefore, the RST controller can ensure a correct robustness against

978-1-4244-1766-7/08/$25.00 ©2008 IEEE

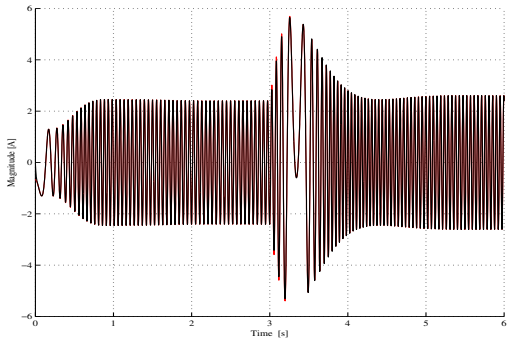

Fig. 12. Dynamic behavior of the first sub-stator current i_{sa_1} (black) and its reference $i^*_{sa_1}$ (red) with uncertainties of $+20\%$ on the stator self-magnetizing inductance, of $+80\%$ on the viscous friction and of -50% on the inertia.

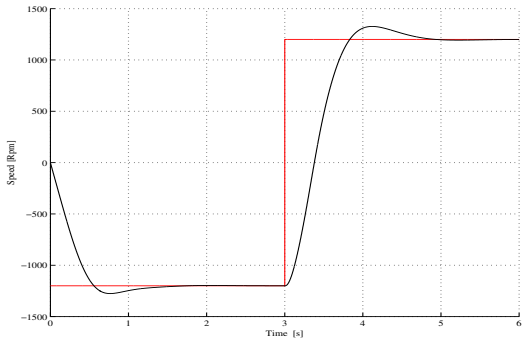

Fig. 13. Dynamic behavior of the mechanical speed (black) versus its reference (red) with uncertainties of $+20\%$ on the stator self-magnetizing inductance, of $+80\%$ on the viscous friction and of -50% on the inertia.

uncertainties of parameters of the motor. In practice, this fact is important because it is impossible to have an exact value of each parameter of the machine.

V. Conclusion

In this investigation, one shows the application of RST controller on the vector control of the double-star induction machine. Results show correct performances of the controller in term of reference tracking and disturbance rejection even under some uncertainties of electrical and mechanical parameters of the motor. These results are very important in industrial application because, generally, the electrical parameter such as the stator resistance varies with the temperature, the inductance may change with the aging of the motor. The mechanical parameters may also be affected by the aging of the system. These situations involve need of more robust controllers. These studies prove that the RST controller can offer a satisfactory performances. Our second paper shows an exemple of experimental implementation of this kind of controller on a complexe system [13]. It is observed in this paper that RST controller gives good results for the control of

References

[1] A.R. Munoz and T.A. Lipo, "Dual stator winding induction machine drive", in *IEEE Transactions on Industrial Application*, vol. 36, pp. 1369– 1379, September/October. 2000.

[2] G. Dong and O. Ojo, "Efficiency Optimizing Control of Induction Motor Using Natural Variables", in *IEEE Transactions on Industrial Electronic*, vol. 53, no. 6, pp. 1791-1798, December 2006.

[3] E. Levi, "Multiphase Electric Machines for Variable-Speed Applications", *IEEE Transactions on Industrial Electronics*, vol. 55, no. 5, pp. 1893–1909, May 2008.

[4] H. Razik, A. Rezzoug and D. Hadiouche, "Modeling and Analysis of Dual-Stator Induction Motors", in *IEE journal Industrial Application Society*, vol. 125-D, no. 12, pp. 1093-1104, 2005.

[5] D. Hadiouche, H. Razik and A. Rezzoug, "On the Modeling and Design of Dual-Stator Windings to Minimize Circulating Harmonic Currents for VSI Fed AC Machines", in *IEEE Transactions on Industrial Application*, vol. 40, no. 2, pp. 506–516, March/April 2004.

[6] K. Marouani, L. Baghli, D. Hadiouche, A. Kheloui and A. Rezzoug, "Discontinuous SVPWM Techniques for Double Star Induction Motor Drive Control", in *IEEE Annual Conference of the Industrial Electronics Society IECON*, Paris, November 2006.

[7] R. Bojoi, G. Griva and. Profumo, "Field-oriented control of dual three-phase induction motor drives using a Luenberger Flux Observer", in *IEEE Industrial Application Society Annual Meeting*, vol. 3, pp. 1253-1260, Tampa-Floride, October 2006.

[8] R. Bojoi, M. Lazarri, F. Profumo and A. Tenconni, "Digital field-oriented control for dual three-phase induction motor drive", in *IEEE Transactions on Industrial Application*, vol. 39, no. 3, pp. 752–760, May/june 2003.

[9] R.O.C. Lyra and T.A.Lipo, "Torque density improvement in a sixphase induction motor with third harmonic current injection", in *IEEE Industrial Application Society Annual Meeting*, pp. 1779-1786, Chicago II, September/october 2001.

[10] M.A.E. Alali, Y.A. Chapuis, S. Saadate and F. Braun , "Advanced common control method for shunt and series active compensators used in power quality improvement", in *IEE Electric Power Applications*, vol. 151, no. 6, pp. 658–665, Novemeber 2004

[11] G.F. Franklin, J.D Powell and M.L Workman, "Digital Control of Dynamic Systems," Addison-Wesley, Reading, 1998.

[12] K. Ogata, "Discrete-Time Control Systems", Second edition, Prentice hall, New Jersey, USA-1994.

[13] R.N. Andriamalala, H. Razik, L. Baghli and F.M. Sargos, "Digital Vector Control of a Six-Phase Series-Connected Two-Motor Drive", in *IEEE Annual Conference of the Industrial Electronics Society IECON*, November 10-13, 2008, Orlando, Florida, USA, 6pp.